Progress In Electromagnetics Research M, Vol. 89, 83–92, 2020

Miniaturized Quintuple Band Antenna for Multiband Applications

Fouad Fertas[1, *], Mouloud Challal[1], and Khelil Fertas[2]

Abstract—This paper presents a miniaturized quintuple band antenna for multiband operation with the aim of developing a small and simple structure antenna that can operate at multiband frequency. The proposed antenna contains a rectangular microstrip patch, a transmission line with 50 Ω coplanar waveguide (CPW), and six L-slots. By introducing these L-slots along the X and Y axis, in the radiating element, the antenna yields five resonance modes at 2.4, 3.5, 4.4, 6.09, and 7.7 GHz while keeping the size of $27.4 \times 24\,\text{mm}^2$. The prototype of the proposed antenna is constructed and experimentally studied. The measured and simulated results prove that the proposed multiband antenna is suitable for Bluetooth, WLAN, WiMAX, LTE, and X band applications. The antenna is designed using FR4 lossy substrate material with relative permittivity of 4.4 and thickness of 1.6 mm.

1. INTRODUCTION

Multiband antenna actually has a lot of significance in cognitive and multiservice radios, and integrating a large number of bands into one antenna becomes necessary and important in various applications. Conventional WLAN/WiMAX frequency bands can be classified into three major bands: 2.4–2.7 GHz, 3.3–37 GHz, and 5.15–5.85 GHz [1]. In addition, the frequency bands used almost coincide, and scientists have attempted to make improvement and prevent interference. Currently, most wireless communication devices are in low profile, easy and inexpensive to manufacture, so the designed antenna should focus on multiple frequency bands covering S (2–4 GHz), C (4–8 GHz), X (7–12 GHz) bands and small structures that are simple and easy to manufacture. In the integration of more than one standard into same compact antenna, the optimization difficulty increases, and there are many techniques for achieving multiband antennas, such as the use of L, T, U, and V-shaped slots cutting off from the top of the radiating element of an antenna [2–6], slots at rectangular radiating patch with partial ground plane or defected ground plane using L U-shaped slots [7, 8]. Use a patch antenna with inclined slots, tow grooves in the form of a rectangle on the circular surface of the disk, with an asymmetry gap of the coplanar waveguide (CPW) feeding structure [9], and a multi-branch structure is used in [10], whose each branch is tuned according to the resonance length of the desired frequency band and the coupling of each resulting branch into different bands. A slot enclosed in a rectangular patch in the form of a rectangular split-ring is used in [11, 12], and a radar composed of two branches and a short stub is used in [13], but few internal multi-band antennas can cover more than three bands, including both WiMAX and WLAN bands [14–22].

In this article, we present a CPW-fed antenna that uses L-shaped slots in the radiating element to generate five frequency bands. The antenna includes a rectangular radiating element and L-shaped slots with distinct dimensions in suitable places cut off from the radiating element; the antenna is supplied by the CPW coplanar waveguide technique. Its structure is designed on a single metal side of an FR4 substrate. L-shaped slots are positioned in the radiating element in well studied locations to affect

Received 19 November 2019, Accepted 11 January 2020, Scheduled 30 January 2020

* Corresponding author: Fouad Fertas (f.fertas@univ-boumerdes.dz).

[1] Signals and Systems Laboratory, Institute of Electrical and Electronic Engineering, University M'hamed BOUGARA of Boumerdes, Algeria. [2] Ecole Nationale Polytechnique, Electronics Department, El-Harrach Algiers, Algeria.

the current density, enabling the suggested design to function at five frequency bands (2.36–2.58 GHz), (3.07–4.01 GHz), (4.25–5.27 GHz), (5.9–6.29 GHz), and finely (7.01–8.1 GHz) to cover WiMAX also known as IEEE 802.16 with its three allocation frequency bands which are: low band (from 2.4 to 2.8 GHz), middle band (from 3.2 to 3.8 GHz), and high band (from 5.15 to 5.75 GHz), Bluetooth (2.4–2.48 GHz), LTE (2.384–2.574, 3.2–3.3 GHz), WLAN (2.4–2.48 GHz), and WLAN bands at 3.6 GHz (802.11y), 4.9 GHz (802.11y public safety WLAN), 5 GHz (802.11 a/h/j/n/ac), 5.9 GHz (801.11 p) bands, and 7.7 GHz for X band.

2. ANTENNA DESIGN AND CONFIGURATION

In this section, the geometric design of the proposed structure is discussed in detail, for the configuration of an antenna that covers five sub-bands for WiMAX/WLAN standard and also other multiband applications. The concept of designing this antenna is based on an L-shaped slots monopole antenna structure.

2.1. Antenna Configuration

Figure 1 shows the evolution process for the proposed antenna configuration, and the antenna is printed on the front face of the dielectric substrate FR4 of thickness 1.6 mm with a relative permittivity ε_r of 4.4 and dielectric loss tangent of 0.02. The total substrate footprint ($L_{sub} \times W_{sub}$) of the antenna is ($27.4 \times 24\,\text{mm}^2$), and the radiating patch is constructed as a simple rectangle with dimensions ($L_p \times W_p$) of ($14 \times 16\,\text{mm}^2$). The antenna is supplied by CPW technique. The optimized physical values of the antenna parameters are listed in Table 1.

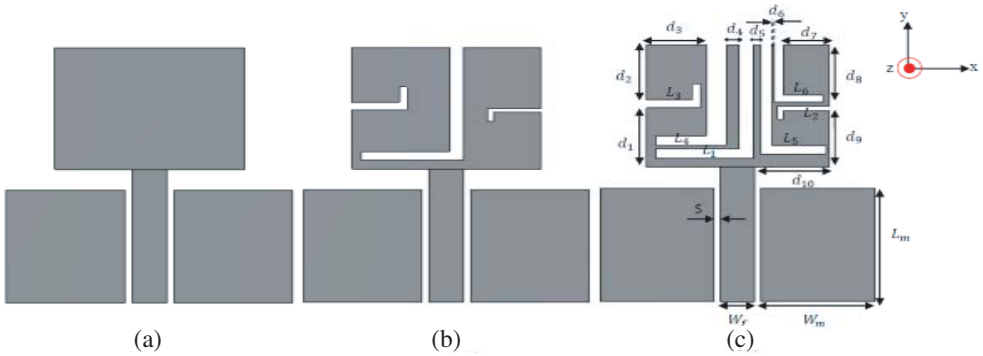

Figure 1. Investigated design process of L shaped slots antenna, (a) reference antenna, (b) three slots cutaway from the patch rectangle, (c) six L slots cutaway from the patch rectangle (final design).

2.2. Design Procedure

Figure 1 displays the design evolution process, initially, using the standard transmission line equations as a guide whose purpose is to design a conventional microstrip patch fed by CPW line. Therefore, as shown in Figure 1(a), this is the first step in the suggested antenna design method, and a reference antenna (RA) is then acquired. We start by designing a conventional multiband patch antenna (MPA) by identifying the patch antenna dimensions. Width and length of the antenna are then calculated as $W_P = 16\,\text{mm}$ and $L_P = 14\,\text{mm}$, in order to have a response $f_r = 3.5\,\text{GHz}$, which is considered as the first step to configure the proposed multiband antenna. A full wave electromagnetic CST MWS simulator is used to simulate and analyze the multiband antenna. Figure 2 shows the simulated return loss results for our designed multiband antenna, and the antenna designed by this technique has a single resonance frequency at $f_r = 3.6\,\text{GHz}$, with $-10\,\text{dB}$ S_{11}. The bandwidth is 3.91 GHz (from 3.05 GHz to 6.96 GHz), and gain is 2.31 dBi. It has an omnidirectional radiation pattern appropriate for wireless communication applications.

Table 1. Optimized parameters of the proposed antenna.

Dimension	Length (mm)	Dimension	Length (mm)
d_1	6.8	W_m	10
d_2	6.3	L_m	13
d_3	5.2	S	0.58
d_4	1.3	W_f	2.94
d_5	0.5	$L_{11}L_{12}L_{13}L_{14}$	$13, 8.7, 1, 1.2$
d_6	0.2	$L_{21}L_{22}L_{23}L_{24}$	$4.5, 1.3, 0.5, 0.5$
d_7	4	$L_{31}L_{32}L_{33}L_{34}$	$4.7, 2.9, 0.7, 0.9$
d_8	7	$L_{41}L_{42}L_{43}L_{44}$	$11.5, 6, 1.1, 1.8$
d_9	6.5	$L_{51}L_{52}L_{53}L_{54}$	$12.2, 3.5, 1, 1$
d_{10}	6.52	$L_{61}L_{62}L_{63}L_{64}$	$6.5, 4.3, 0.8, 0.8$

Furthermore, L-shaped slot L_1 is positioned in the center of the rectangle's top rib, and two other L-shaped slots L_2 and L_3 are also incorporated into the radiating components, with the first positioned in the center of the rectangle's right rib. While the second one is placed in the center of the rectangle's left rib as shown in Figure 1(b), the antenna response will have two frequency bands. The first is a wide band (2.7–5.3 GHz), and the second is narrow band at 6 GHz. However, both of WiMAX with low frequency band (from 2.4 to 2.8 GHz) and high frequency band (from 5.2 to 5.8 GHz) are not covered. Figure 3 shows the simulated return loss corresponding to (Figure 1(b)).

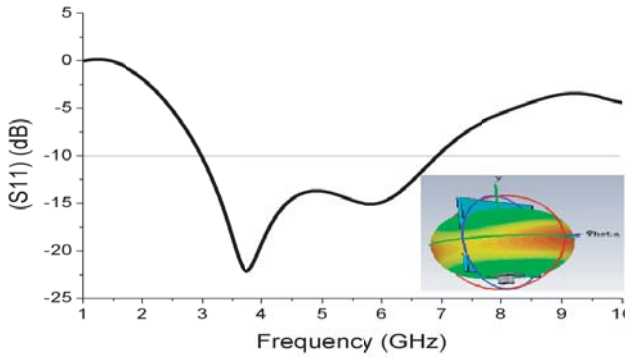

Figure 2. Simulated S_{11} plot and radiation pattern for the conventional CPW-fed antenna, (Figure 1(a)).

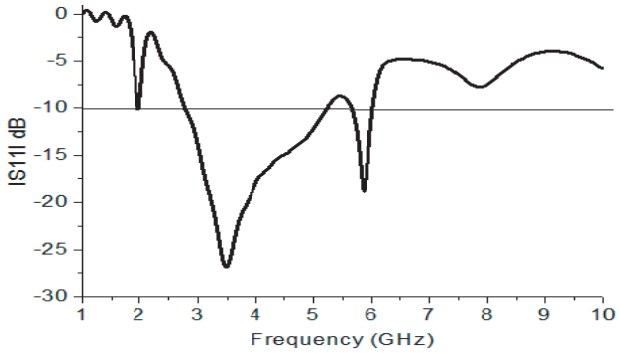

Figure 3. Simulated S_{11} for second antenna, (Figure 1(b)).

The challenge is to add the WiMAX band to the antenna response or to make the antenna radiate in this band while maintaining the previous bands, with the size of the antenna remaining fixed. To avoid the phenomenon of interference, an L-shaped slot L_4 is positioned at the left side of the radiating element, and we note that there is a slight change in S_{11} with the appearance of a new frequency band centered at 2 GHz.

Similarly, an L-shaped slot L_5 introduced in the right side, with this technique and the frequency band centered at 2 GHz, is now centered at 2.7 GHz with a remarkable shift of the other frequency bands, with the appearance of another frequency band centered at 7.8 GHz. An L-shaped slot L_6 is inserted on the right side of the radiating element above L_2, which makes it possible to obtain a new frequency band centered at 4.8 GHz, and during the design of the geometry of the proposed antenna, frequency bands are controlled by adjusting the size of each L-shaped slot according to Equation (1).

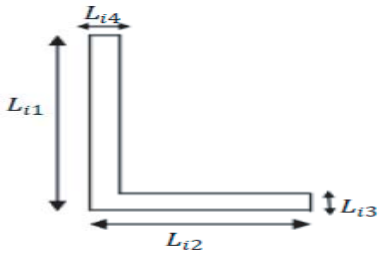

Figure 4. Geometry of L_{ij}-slot, i indicates the number of L-slot and j indicates the dimensions of L-slot number i.

The sizes of L-shaped slots are calculated as the sum of the perpendicular segment length plus the horizontal segment length. Figure 4 shows the layout of L-shaped slot dimensions.

$$\text{Slot length} \approx \frac{3 \times 10^8}{4 f_n \sqrt{((\varepsilon_r+1)/2)}} \tag{1}$$

where ε_r and f_n are dielectric constant of the substrate and a desired frequency respectively, and the slot length implies the perpendicular length rib plus the horizontal length rib of the L-shaped slot.

3. RESULTS AND DISCUSSION

The suggested antenna is intended and simulated using CST microwave studio software V2016 to determine the various parameters and to comprehend the conduct of the suggested antenna. The final antenna prototype is then manufactured and tested using an Agilent HP 8719ES Vector Network Analyzer (VNA) operating in the 100 KHz–20 GHz frequency band.

3.1. Return Loss

In this subsection, the influence of geometric parameter for a return loss is discussed and investigated in details. Figure 5 shows the S_{11} plot for different geometric parameters. Simulated results of the proposed antenna show that the proposed antenna is able to produce five separate frequency bands with -10 dB return loss, which are acceptable values for the antenna to work efficiently for practical wireless applications. The proposed antenna performance is related to the antenna geometry, and changing various geometry parameters makes it possible to adjust to resonate at the desired frequencies. All geometric parameters are optimized with respect to the desired frequency bands. Some parameters have a considerable effect on the antenna characteristics compared to the others, because a small change in the size of one of these parameters affects multiple bands at the same time, and therefore, the independent control of the frequency bands is extremely difficult. Five frequency bands and six slots of antenna make that one or more frequency can be controlled by several slots. Wherefore the variation in parameters is limited to L_1, L_2, L_4 and L_6, and they are studied by varying their length (the change is in the length of the perpendicular segment or the horizontal segment of the L-slot) while the others are fixed. According to Figure 5(a) a small change in the horizontal segment of L_1-slot (L_{12}) with 0.1 mm affects the lowest frequency band 2.4 GHz. This means that when decreasing the slot size L_1, the center of the frequency band shifts to high frequencies, and inversely, when the size of L_1 increases with 0.1 mm, it is found that the frequency band shifts to low frequencies and a risk rising above the -10 dB bar.

In order to avoid redundancy, a recapitulation study in the following points,

- Frequency band (3.07–4.01 GHz): $L_{11} \pm 0.3$ mm, Figure 5(b).
- Frequency band (4.25–5.27 GHz): $L_{62} \pm 0.3$ mm, Figure 5(c).
- Frequency band (5.9–6.29 GHz): $L_{22} \pm 0.1$ mm, Figure 5(d).
- Frequency band (7.01–8.1 GHz): $L_{42} \pm 0.35$ mm, Figure 5(e).

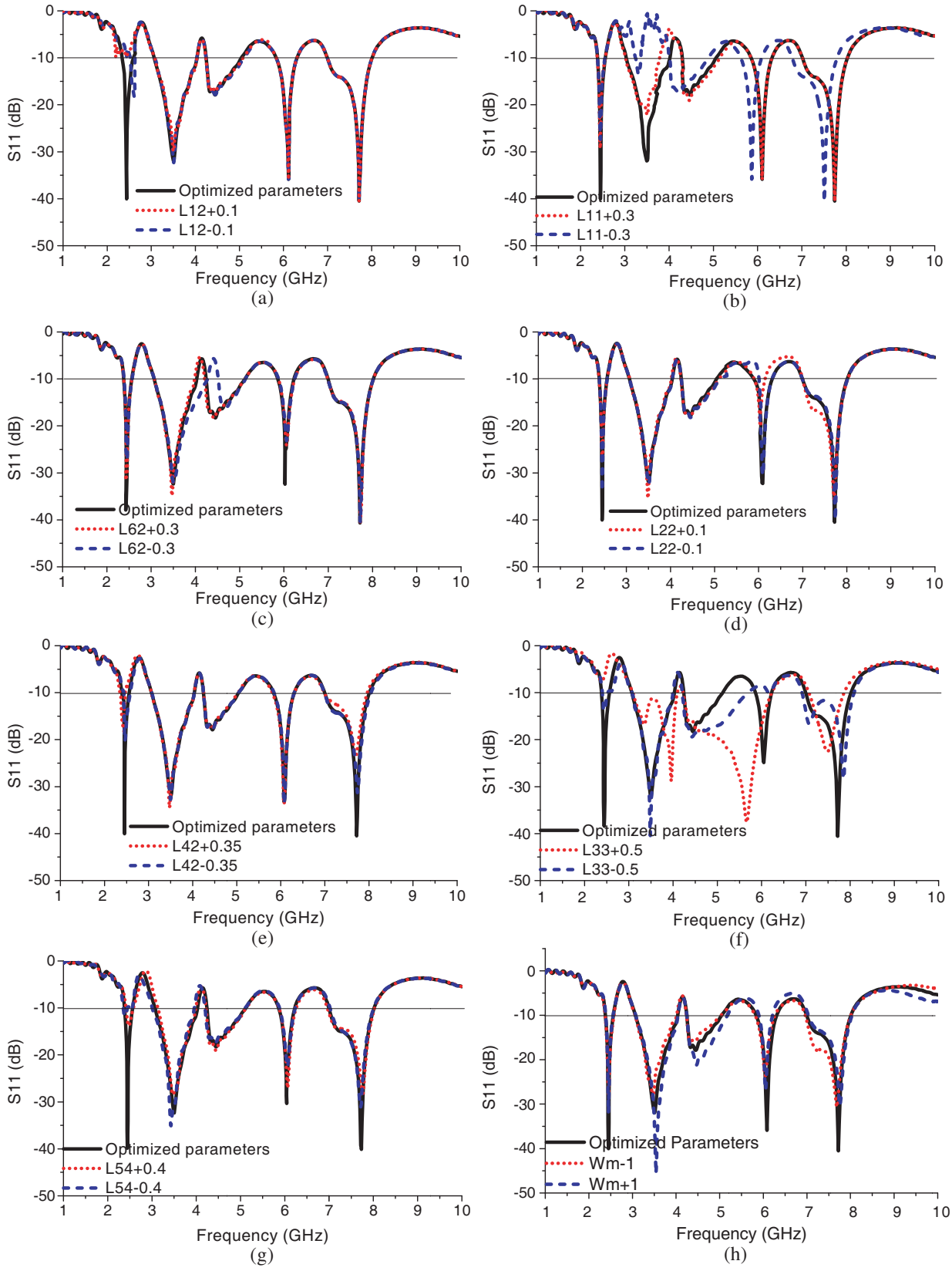

Figure 5. Influence of different geometric parameters at return loss, (Figure 1(c)).

The width of slots L_{i3}, L_{i4} are also optimized in order to achieve a good impedance matching of the proposed slot antenna. Figure 5(f) exhibits the effects of the width L_{33} slot on the return loss characteristics. It is observed that when L_{33} increases a bandwidth of the second and third frequency bands is enhanced, but a remarkable mismatch of the first and forth resonance frequencies is observed, while L_{54} affects the lower frequency band as shown in Figure 5(g). Figure 5(h) shows the influence of the ground plane width. When the size of the ground plane increases, we find that there is a good adaptation of the second and third bands, but the other bands are not well adapted.

3.2. Surface Current Distribution

To further investigate the operating antenna mechanism and clarify the return loss performance of the proposed antenna structure, the current distributions are simulated at the five different resonant frequencies of 2.4, 3.5, 4.4, 6.09, and 7.7 GHz as depicted in Figure 6. It is observed that at the first resonant frequency 2.4 GHz the current intensity is around slots L_1, L_4, L_5 and to a lesser extent around L_2 and L_3, and consequently, this resonant frequency can be controlled by adjusting the length of one of the L slots indicated before. At the second frequency band 3.5 GHz the current is most concentrated between the perpendicular segment of L_1 and the perpendicular segment of L_5 more precisely between L_{11} and L_{51} so that this frequency can be controlled by the size adjustment of either L_{11} or L_{51}. Concerning the third frequency band Figure 6(c) shows that the current is highly concentrated around L_2 which implies that this frequency is controlled by changing the slot size L_2. Figure 6(d) illustrates the current distribution for the fourth frequency band. It is found that the current is highly concentrated around L_2 implying that this frequency band can be controlled by changing the size of L_2. For the last frequency band in Figure 6(e) the current is strongly concentrated all around L_4 which implies that this frequency band can be controlled by changing the size of L_4.

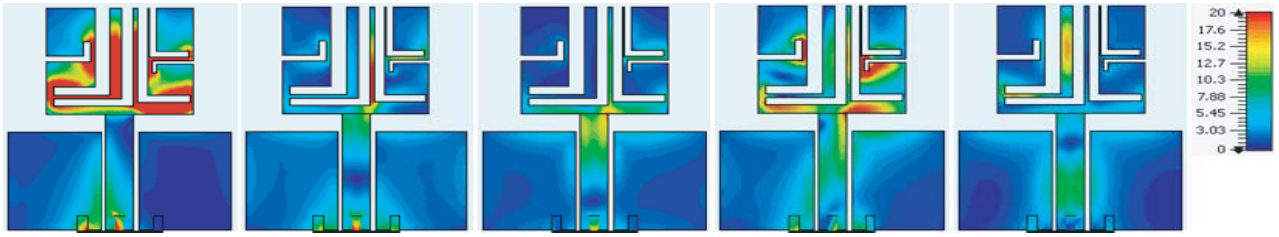

Figure 6. Simulated results of the surface current distributions at all frequencies for the proposed antenna from the left to rights hand side plots are for the frequencies of 2.4, 3.5, 4.4, 6.09, and 7.7 GHz.

3.3. Peak Gain and Efficiency

The simulated antenna peak gains and axial ratio against frequency are shown in Figure 7. The gain at 2.45 GHz is about 1.4 dBi, and the maximum value is around 2.92 dBi at 7.7 GHz. The axial ratio at 2.45 GHz is 8 dB and 5 dB at 7.7 GHz, and the efficiencies of 57%, 94.8%, 91.7%, 75% and 78% are at the operating frequencies 2.4, 3.5, 4.4, 6.09, and 7.7 GHz, respectively. The gains and efficiency of the proposed antenna within the operating bands are sufficient to satisfy the multiband system requirement.

4. EXPERIMENTAL RESULTS

To validate the obtained results, the antenna prototype is fabricated and tested. A photograph of the fabricated antenna is shown in Figure 8, where the simulated and the measured results of the return losses are presented in Figure 9.

From Figure 9 we observe that there is a good agreement between measured and simulated results, with slit differences. These small discrepancies are due to the fabrication tolerance, mismatch of fed connector, and measurement circumstance.

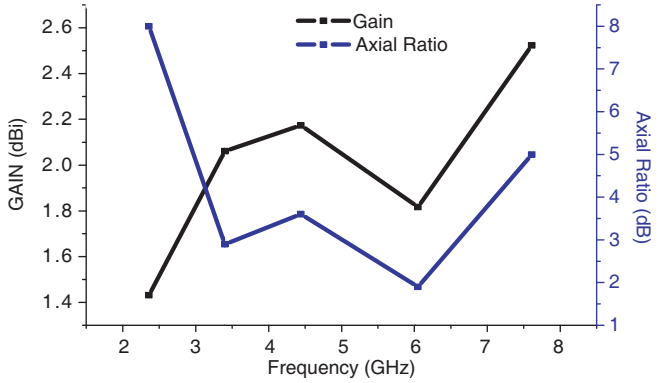

Figure 7. Peak gain in black color and Axial Ratio blue of the proposed antenna.

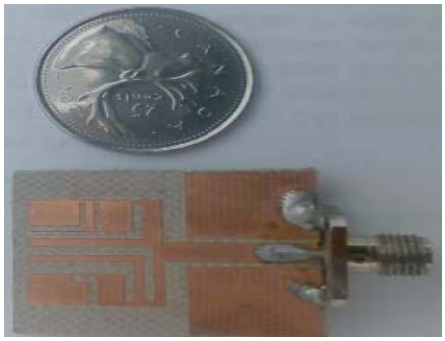

Figure 8. Fabricated antenna.

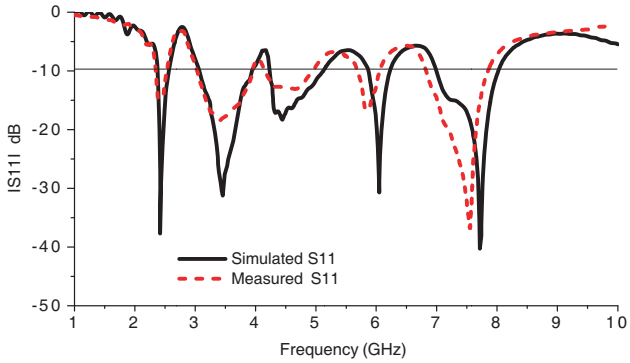

Figure 9. Simulated solid and measured dash returned loss of the proposed design.

Table 2. Comparison of the suggested antenna with other multiband antennas.

Reference	Frequencies band	size (mm^2)	Operating frequency bands (GHz)	Bandwidth (%)	Peak Gain (dBi)
[23]	Four bands	30 × 32	2.38–2.57, 3.29–3.71, 5.09–5.3, 5.7–5.8	7.9, 12,14, 3.9, 1.73	-
[24]	Four bands	30 × 40	1.73–1.9, 2.3–2.7, 3.31–3.68, 5.03–5.93	13, 15, 10.57, 16.3	0.5, 2.8, 1.8 and 3
[25]	Three bands	30 × 34	1.92–2.17, 3.4–3.6, 5.15–5.35	12.5, 5.71, 3.84	−1, 1, 3.5
[26]	Four band	30 × 40	2.36–2.65, 4.28–4.82, 5.47–6.0, 7.28–8.06	11.06, 12, 9.29, 10	2.13, 2.27, 2.56 and 5.33
[27]	Dual band	30 × 30	2.34–2.4, 5.26–5.4	8.3, 2.4	0.64 and 1.2
[28]	Dual band	36 × 39	1.6–2.95, 5.4 6.4	59.34, 16.95	−3.25 and −4.53
[29]	Dual band	40 × 40	2.4–2.48, 5.15–5.8	7.3, 26	0.74 and 2.3
This work	Five bands	27.4 × 24	2.36–2.6, 3.1–4, 4.25–5.27, 5.9–6.3, 7–8.1	9.16, 28.7, 23.18, 6.45, 14.2	1.41, 2.1, 2.3, 1.82, 2.92

4.1. Radiation Pattern

Figure 10 shows the measurement radiation pattern. Figure 10(a) presents the measurement procedure on an anechoic chamber, and Figure 10(b) shows the measured and simulated radiation patterns at all frequencies in H plane and E plane.

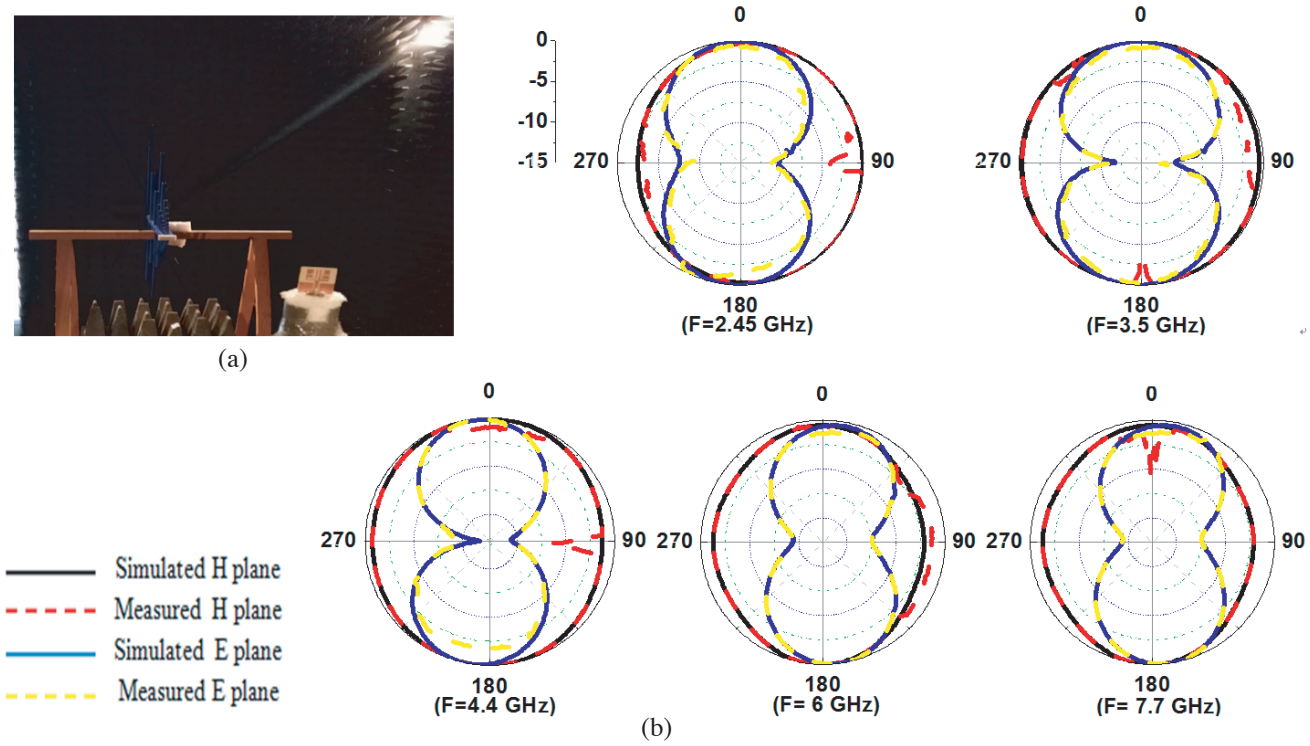

Figure 10. Radiation pattern (a) measurement procedure, (b) measured and simulated in H-plane and E-plane at frequencies 2.45, 3.5, 4.4, 6.09 and 7.7 GHz.

A good agreement between them is noted. The figure obviously demonstrates that the antenna has an almost omnidirectional radiation pattern in H plane at all frequencies and bidirectional radiation pattern in E plane.

5. COMPARATIVE STUDY

The performance comparison of the proposed multiband antenna with those reported in recent works is illustrated in the Table 2. The conducted study demonstrates that the proposed antenna provides size miniaturization and good performances in terms of bands number, bandwidth, and peak gain.

6. CONCLUSION

This paper proposes a multiband antenna for the use in different applications. In order to add more functionality to the antenna, six L-slots have been inserted in the radiating element. Complete analysis of the geometrical parameters is performed, detailed design considerations for the antenna described, and effects of various parameters on these modes are analyzed as well. The impedance bandwidth covers several resonant frequencies in the ranges of (2.36–2.58 GHz), (3.07–4.01 GHz), (4.25–5.27 GHz), (5.9–6.29 GHz), and (7.01–8.1 GHz). The multiband nature, simple structure, small size, and good omnidirectional radiation pattern make this antenna an excellent candidate for Bluetooth, 2.4/5.8 GHz WLAN, 2.5/5.15 GHz WiMAX wireless standards, 5.9 GHz ITS band (5.85–5.925 GHz), and X-band satellite communication.

ACKNOWLEDGMENT

This work is supported by the "Direction Générale de la Recherche Scientifique et du Développement Technologique (DGRSDT)".

REFERENCES

1. Chaimool, S. and P. Akkaraekthalin, *CPW-fed Antennas for WiFi and WiMAX*, A. T. T. in WiMAX, R. Hincapie, ed., ISBN: 978-953-307-965-3, In Tech, Available from: http://www.intechopen.com/books/advenced-transmission-techniques in-wimax/cpw-fed-antennas-for wifi-and-wimax.
2. Saadh, A. W. M. and R. Poonkuzhali, "A compact CPW fed multiband antenna for WLAN/INSAT/WPAN applications," *AEU — International Journal of Electronics and Communications*, Vol. 109, 128–135, 2019.
3. Khidre, A., et al., "Wide band dual-beam U-slot microstrip antenna," *IEEE Transactions on Antennas and Propagation*, Vol. 61, No. 3, 1415–1418, 2013.
4. Ali, T. and R. C. Biradar, "A triple-band highly miniaturized antenna for WiMAX/WLAN applications," *Microwave and Optical Technology Letters*, Vol. 60, No. 2, 466–471, 2018.
5. Khan, M. U. and M. S. Sharawi, "A 2×1 multiband MIMO antenna system consisting of miniaturized patch elements," *Microwave and Optical Technology Letters*, Vol. 56, No. 6, 1371–1375, 2014.
6. Saadh, A. W. M., R. Poonkuzhali, and T. Ali, "A miniaturized single-layered branched multiple-input multiple-output antenna for WLAN/WiMAX/INSAT applications," *Microwave and Optical Technology Letters*, 1–7, 2019.
7. Moosazadeh, M. and S. kharkovsky, "Compact and small planar monopole antenna with symmetrical L- and U-shaped slots for WLAN/WiMAX applications," *IEEE Antennas and Wireless Propagation Letters*, Vol. 13, 388–391, 2014.
8. Chetal, S., A. K. Nayak, and R. K. Panigrahi, "Multiband antenna for WLAN, WiMAX and future wireless applications," *2019 URSI Asia-Pacific Radio Science Conference (AP-RASC)*, 1–4, New Delhi, 2019.
9. Kim, I., K. Min, J. Jeong, and S. Kim, "Circularly polarized tripleband patch antenna for non-linear junction detector," *2013 Asia-Pacific Microwave Conference Proceedings*, 140–142, Nov. 5–8, 2013.
10. Chuang, C.-S., Y.-J. Jhang, and T.-T. Ku, "Compact multi-broadband monopole antenna for integrated mobile broadband wireless radio access system application," *2012 Asia Pacific Microwave Conference Proceedings*, 598–600, Dec. 4–7, 2012.
11. El Misilmani, H. M., M. Al-Husseini, K. Y. Kabalan, and A. El-Hajj, "A simple miniaturized triple-band antenna for WLAN/WiMAX applications," *PIERS Proceedings*, 608–612, Moscow, Russia, Aug. 19–23, 2012.
12. Sun, X. L., J. Zhang, S. W. Cheung, and T. I. Yuk, "A triple-band monopole antennas for WLAN and WiMAX applications," *APSURSI*, 1–2, 2012.
13. Patel, U. and T. Upadhyaya, "Design and analysis of μ-negative material loaded wideband electrically compact antenna for WLAN/WiMAX applications," *Progress In Electromagnetics Research M*, Vol. 79, 11–22, 2019.
14. Fertas, F., M. Challal, and K. Fertas, "Design and implementation of a miniaturized CPW-fed miscrostrip antenna for triple-band applications," *2017 5th International Conference on Electrical Engineering — Boumerdes (ICEE-B)*, Boumerdes, Algeria, IEEE, Oct. 29–31, 2017, DOI: 10.1109/ICEE-B.2017.8192103.
15. Fertas, K., H. Kimouche, M. Challal, F. Ghanem, F. Fertas, and R. Aksas, "Development of a novel UWB planar antenna using a genetic algorithm," *2017 5th International Conference on Electrical Engineering — Boumerdes (ICEE-B)*, Boumerdes, Algeria, IEEE, Oct. 29–31, 2017, DOI: 10.1109/ICEE-B.2017.8192102.

16. Fertas, K., H. Kimouche, M. Challal, H. Aksas, and R. Aksas, "Multiband microstrip antenna array for modern communication systems," *2015 4th International Conference on Electrical Engineering (ICEE)*, Boumerdes, Algeria, IEEE, Dec. 13–15, 2015, DOI: 10.1109/INTEE.2015.7416757.
17. Fertas, K., H. Kimouche, M. Challal, H. Aksas, R. Aksas, and A. Azrar, "Design and optimization of a CPW-fed tri-band patch antenna using genetic algorithms," *ACES — Applied Computational Electromagnetics Society Journal*, Vol. 30, No. 7, Jul. 2015.
18. Djafri, K., M. Challal, R. Aksas, M. Dehmas, F. Mouhouche, and J. Romeu, "A novel miniaturized dual-band microstrip antenna for WiFi/WiMAX applications," *2017 5th International Conference on Electrical Engineering — Boumerdes (ICEE-B)*, Boumerdes, Algeria, IEEE, Oct. 29–31, 2017, DOI: 10.1109/ICEE-B.2017.8192084.
19. Kumar, A., J. K. Deegwal, and M. M. Sharma, "Design of multi-polarised quad-band planar antenna with parasitic multistubs for multiband wireless communication," *IET Microwaves, Antennas and Propagation*, Vol. 12, No. 5, 718–726, Apr. 2017.
20. Malek, M. A., S. Hakimi, S. K. A. Rahim, and A. K. Evizal, "Dual band CPW-fed transparent antenna for active RFID tags," *IEEE Antennas and Wireless Propagation Letters*, Vol. 14, 919–922, 2015.
21. Li, Q. L., S. W. Cheng, D. Wu, and T. I. Yuk, "Optically transparent dual-band MIMO antenna using micro-metal mesh conductive film for WLAN system," *IEEE Antennas and Wireless Propagation Letters*, Vol. 16, 920–923, 2017.
22. Mezache, Z., C. Zara, and F. Benabdelaziz, "Design of a novel chiral fractal resonator," *S. J. of Ele. Engineering*, Vol. 16, No. 3, 377–385, Oct. 2019.
23. Ávila, D. R., Y. P. Marrero, A. S. Vera, F. M. Rizo, J. V. Sanz, and A. T. Puente, "Printed quad-band CPW-fed slot antenna," *Microwave and Optical Technology Letters*, Vol. 58, No. 1, 145–151, 2016.
24. Honarvar, M. A., N. Hamidi, and B. S. Virdee, "Multiband antenna for portable device applications," *Microwave and Optical Technology Letters*, Vol. 57, No. 4, 956–959, 2015.
25. Challal, M., F. Mouhouche, K. Djafri, and A. Boutejdar, "Quad-band microstrip patch antenna for WLAN/WiMAX/C/X applications," *IEEE 2017 5th International Conference on Electrical Engineering — Boumerdes (ICEE-B)*, Boumerdes, Algeria, IEEE, Oct. 29–31, 2017, DOI: 10.1109/ICEE-B.2017.8192065.
26. Kumar, A., J. K. Deegwal, and M. M. Sharma, "Design of multi-polarised quad-band planar antenna with parasitic multistubs for multiband wireless communication," *IET Microwaves, Antennas and Propagation*, Vol. 12, No. 5, 718–726, Apr. 2017.
27. Desai, A., U. Trushit, and P. Merih, "Dual band slotted transparent resonator for wireless local area network applications," *Microwave and Optical Technology Letters*, Vol. 60, No. 12, 3034–3039, 2018.
28. Malek, M. A., S. Hakimi, S. K. A. Rahim, and A. K. Evizal, "Dual band CPW-fed transparent antenna for active RFID tags," *IEEE Antennas and Wireless Propagation Letters*, Vol. 14, 919–922, 2015.
29. Li, Q. L., S. W. Cheung, D. Wu, and T. I. Yuk, "Optically transparent dual-band MIMO antenna using micro-metal mesh conductive film for WLAN system," *IEEE Antennas and Wireless Propagation Letters*, Vol. 16, 920–923, 2017.